ELSEVIER

Biochimica et Biophysica Acta 1561 (2002) 119–128

BIOCHIMICA ET BIOPHYSICA ACTA
BBA

www.bba-direct.com

# The effect of fusion inhibitors on the phase behaviour of *N*-methylated dioleoylphosphatidylethanolamine

Malcolm J.M. Darkes, Thad A. Harroun, Sarah M.A. Davies, Jeremy P. Bradshaw *

*Department of Preclinical Veterinary Sciences, Royal (Dick) School of Veterinary Studies, University of Edinburgh, Summerhall, Edinburgh EH9 1QH, UK*

Received 26 September 2001; received in revised form 10 December 2001; accepted 14 December 2001

**Abstract**

The effects of two fusion inhibitors on the lipid polymorphism of *N*-methylated dioleoylphosphatidylethanolamine were studied using temperature-resolved, small-angle X-ray diffraction. The inhibitory role of the tri-peptide carbobenzoxy-D-phenylalanine-L-phenylalanine-glycine and the lipid 1-lauroyl-2-hydroxy-*sn*-glycero-3-phosphocholine in the fusion pathway was studied, using the non-lamellar phase behaviour of the lipid as a model. We used p15EK, the N-terminal region of gp41 from feline leukaemia virus as promoter of membrane fusion, and measured the structural parameters of each observed lipid phase as a function of temperature. The fusion inhibitors were found to impede the expression of negative curvature of lipid monolayers even in the presence of fusion peptide. The results of this study are interpreted in relation to models of the membrane fusion mechanism. © 2002 Published by Elsevier Science B.V.

*Keywords:* Time resolved X-ray diffraction; Small angle X-ray diffraction; Small angle X-ray scattering; Biomembrane fusion; Inhibitor; Lamellar phase; Cubic phase; Hexagonal phase

## 1. Introduction

Enveloped virus particles require membrane fusion in order to introduce their infective nuclear material into a host cell [1]. Each virus employs specialised, extra-membranous glycoproteins that catalyse the fusion process. These so-called 'fusion proteins' promote the merging of two originally distinct membranes into one. Research has shown that peptides derived from the N-terminus of fusion proteins, exhibit similar membrane fusion activities. We have previously reported that the fusion peptide from feline leukaemia virus (FeLV), p15EK, destabilises the $L_\alpha$ phase and promotes the formation of non-bilayer structures by increasing negative curvature strain [2,3].

Part of the fusion process involves the bending of individual leaflets of both the viral and cell membrane into more tightly curved structures than normally encountered [4]. Current theory states that

Abbreviations: CBZ-D-FFG, carbobenzoxy-D-phenylalanine-L-phenylalanine-glycine; $d_H$, lattice repeat distance (hexagonal phase phospholipid); $d_L$, lattice repeat distance (lamellar phase phospholipid); $d_Q$, lattice repeat distance (cubic phase phospholipid); DOPE-Me, *N*-methylated dioleoylphosphatidylethanolamine; EDTA, ethylenediaminetetraacetic acid; FeLV, feline leukaemia virus; LPC, 1-lauroyl-2-hydroxy-*sn*-glycero-3-phosphocholine; MLV, multilamellar vesicle; p15EK, fusion peptide from spike protein p15E of FeLV; PIPES, 1,4-piperazinediethanesulfonic acid; $q$, $2\pi/d$; SAXS, small-angle X-ray scattering; $T_H$, temperature at which hexagonal phase is first observed; $T_Q$, temperature at which cubic phase is first observed

* Corresponding author. Fax: +44-131-650-6576.
*E-mail address:* j.bradshaw@ed.ac.uk (J.P. Bradshaw).

0005-2736/02/$ – see front matter © 2002 Published by Elsevier Science B.V.
PII: S0005-2736(01)00464-3

monolayer curvature leads to the formation of non-lamellar structures prior to the formation of the fusion pore [5]. Each outer membrane leaflet exhibits negative curvature whilst each inner membrane leaflet exhibits positive curvature during the formation of highly curved intermediates [6,7]. This theory can be tested by altering the lipid composition or by including asymmetrical agents, such as peptides, lysolipids or other molecules that have contrasting effects on membrane curvature strain [4,8,9], and observing changes in the phase behaviour of the lipid.

We report on the effects of the two fusion inhibitors, one protein based, carbobenzoxy-D-phenylalanine-L-phenylalanine-glycine (CBZ-D-FFG), and one phospholipid based, 1-lauroyl-2-hydroxy-sn-glycero-3-phosphocholine (LPC) on the lipid phase behaviour of multilamellar vesicles (MLVs) composed of *N*-methylated dioleoylphosphatidylethanolamine (DOPE-Me).

CBZ-D-FFG is a hydrophobic tripeptide that inhibits the fusion process in a dose-dependent manner [10]. Multinuclear resonance spectroscopy and calorimetric analysis suggest that its interaction with phospholipid membranes account for its mechanism of action. It is thought that CBZ-D-FFG resides within the membrane interface and prevents the formation of highly curved surfaces [11,12]. CBZ-D-FFG raises the lamellar-to-hexagonal phase transition temperature [13] indicating a reluctance of this peptide to be associated with lipids that exhibit negative curvature at lower temperatures.

The detergent LPC forms oil-in-water micellar aggregates when in an excess water condition above its critical micelle concentration. Its large hydrated headgroup and relatively short hydrocarbon chain give the molecule an inverted cone shape. This shape is thought to reduce negative curvature strain of the outer membrane leaflet during the initial stages of the fusion event [14–16].

Lipid mesomorphism was measured by temperature-resolved X-ray diffraction, a quantitatively and qualitatively direct method of characterising lipid phase transitions. Real-time small-angle X-ray scattering (SAXS) images were recorded of pure lipid dispersions and lipid dispersions containing fusion inhibitor as the temperature was progressively increased. Images were also recorded in the presence of a fixed p15EK concentration of 1 mol% in order to evaluate the inhibitors' ability to prevent the formation of inverted lipid phases. This report describes the effect of these inhibitors on lipid structural parameters. Based on the results of this technique, we relate these structural parameters to a proposed mechanism of inhibition.

## 2. Materials and methods

### 2.1. Sample preparation

FeLV (strain C/Sarma, SWISSPROT accession number P06752) contains the fusion peptide p15EK (EPISLTVALMLGGLTVGGIAAGVGTGTK), which was synthesised by Albachem (Edinburgh, UK). CBZ-D-FFG was obtained from Sigma (St. Louis, MO). LPC and DOPE-Me were purchased from Avanti Polar Lipids (Alabaster, AL) and used without further purification.

MLVs were prepared by rehydrating phospholipid films as previously described [8]. The buffer used was 20 mM PIPES, 1 mM EDTA, 150 mM sodium chloride and 0.3 mM sodium azide at pH 7.4. All samples had a low lipid concentration of 100 mM, which is equivalent to 7.57% (w/v) and ensures an excess water condition. The lipid dispersions were then subjected to five freeze–thaw cycles. Repeated freezing and thawing across the chain-melt temperature ensures that the lipid is fully hydrated regardless of the thermal history of the lipid.

### 2.2. Temperature-resolved X-ray diffraction

The X-ray diffraction experiments were performed at station 2.1 of the Synchrotron Radiation Source at Daresbury Laboratory, UK and at the SAXS instrument at Sincrotrone Trieste Elettra, Italy. In both cases, the X-ray wavelength was 0.154 nm. The specimen-to-detector length was approximately 1.5 m. At Daresbury, the sample holder was a Teflon-lined brass chamber with mica windows and an external circulating water bath to control the sample temperature. A thermocouple fixed to the sample chamber monitored the temperature continuously. At Elettra, each sample was contained in a glass capillary tube, held in a steel block with electronic (Peltier device) temperature control. The temperature increased in a

linear fashion at a rate of 30 K/h, a rate at which metastable cubic phase is not normally observed in DOPE-Me. Each frame of data collection lasted for 30 s. The effect of thermal radiation from X-ray beams of this kind was minimal. Aluminium foils were added to attenuate the incident beam until no loss of diffracted intensity was observed throughout the duration of a complete temperature scan.

### 2.3. Data analysis

The raw data were corrected using local programs at each synchrotron. Corrections for sample thickness and variations in detector response were applied and background counts were subtracted. Detector response was determined by measuring a fixed source, $^{59}$Fe, overnight both before and after data collection. Calibration of the *x*-axis for small-angle scattering was achieved by using rat-tail collagen as a standard [17]. This calibration was repeated prior to the exposure of each new sample. The location and intensity of each order of diffraction was given by fitting Lorentzian distributions.

## 3. Results

Fig. 1 shows the variation of lattice repeat distance *d* with temperature, broken down into the different lipid structural phases: L (lamellar), H (hexagonal) and Q (cubic). Fig. 2 is a schematic summary of this phase information, making clearer the phase behaviour of the pure lipid control and MLVs containing p15EK and/or fusion inhibitors, as a function of temperature.

Lipid polymorphism is generally well understood, with the possible exception of specific cubic space-groups, so that although phases should normally be

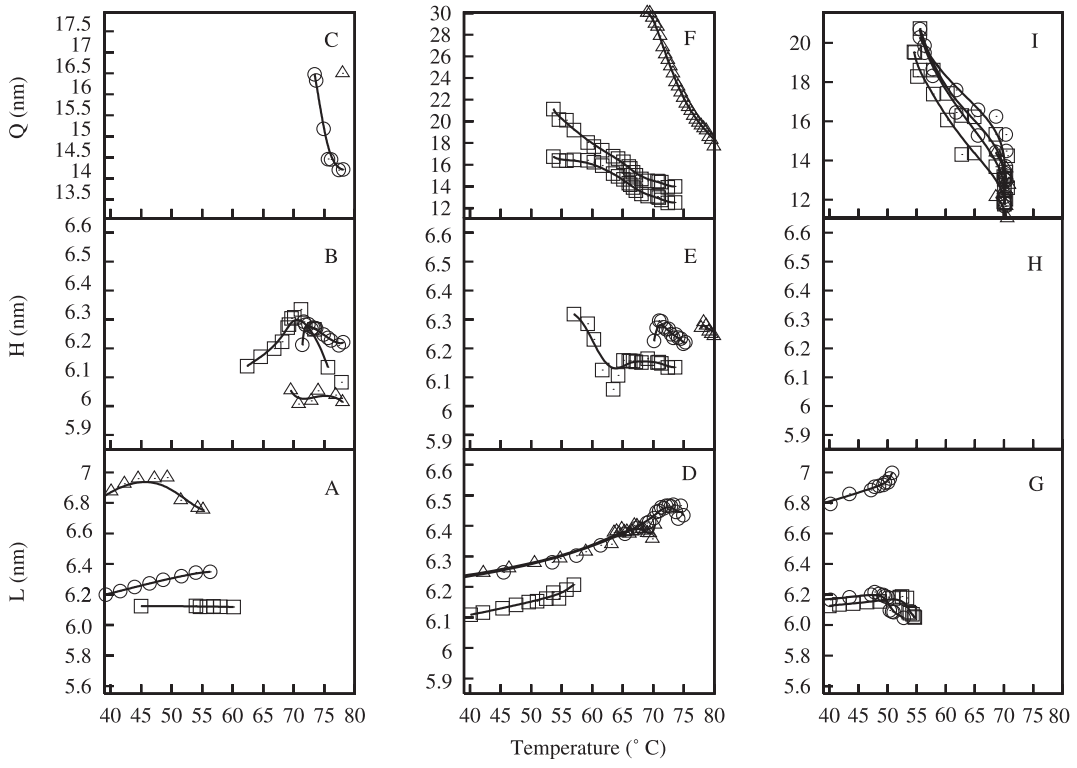


Fig. 1. Change in lattice basis vector lengths (nm) for all observed phases of DOPE-Me with respect to temperature (°C) as determined by time-resolved SAXS performed at station 2.1 of the Synchrotron Radiation Source at Daresbury Laboratory, UK and at the SAXS instrument at Sincrotrone Trieste Elettra, Italy. (A–C) Pure DOPE-Me (□); DOPE-Me, 2 mol% CBZ-D-FFG (○); DOPE-Me, 5 mol% CBZ-D-FFG (△). (D–F) DOPE-Me, 1 mol% p15EK (□); DOPE-Me, 1 mol% LPC (○); DOPE-Me, 1 mol% p15EK, 1 mol% LPC (△). (G–I) DOPE-Me, 1 mol% p15EK with (□) 2 mol%, (○) 5 mol% and (△) 10 mol% CBZ-D-FFG.

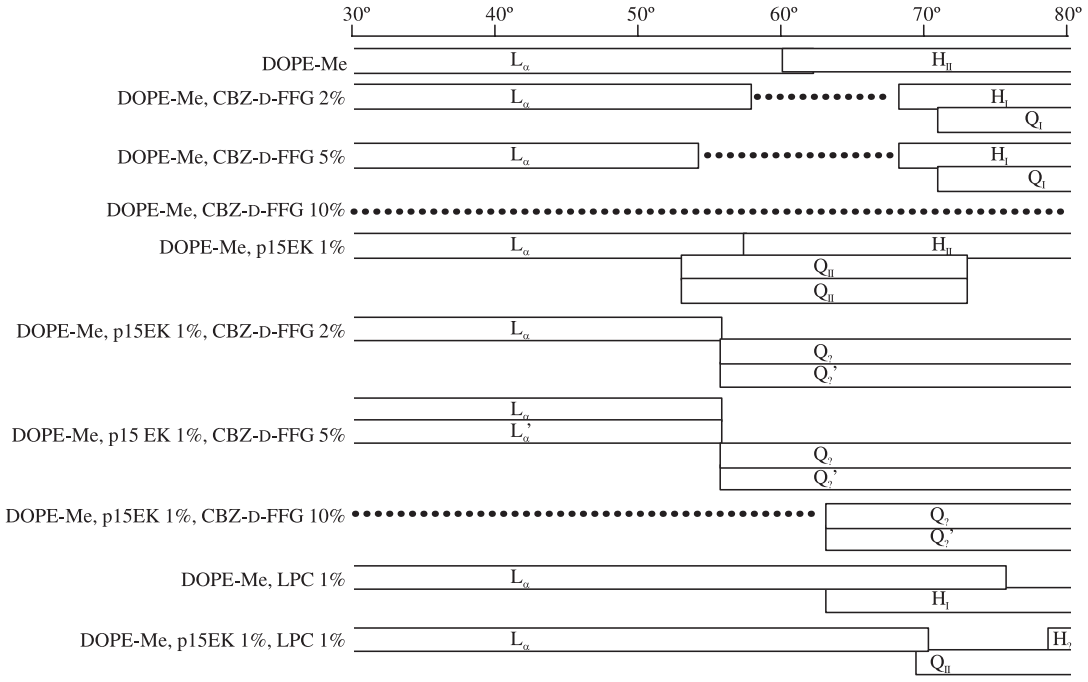


Fig. 2. Schematic summary of the phase behaviour of MLVs of DOPE-Me and DOPE-Me with p15EK and/or fusion inhibitors, as a function of temperature. L (lamellar), H (hexagonal) and Q (cubic). The subscript is I (non-inverted), II (inverted) or ? (unknown). The assignment is described in the text. Dotted line indicates temperatures at which no structure was observed.

identified by assigning an (*h*,*k*,*l*) index to each peak, even SAXS data with few unique orders of diffraction can be unambiguously assigned. Diffraction peaks from the lamellar, hexagonal and higher order cubic potentially overlap each other in the region of $q = 0.9$ to 1.1 $nm^{-1}$. However, in those cases where there was coexistence of lamellar and hexagonal, the latter could easily be distinguished by its unique $\sqrt{3}$

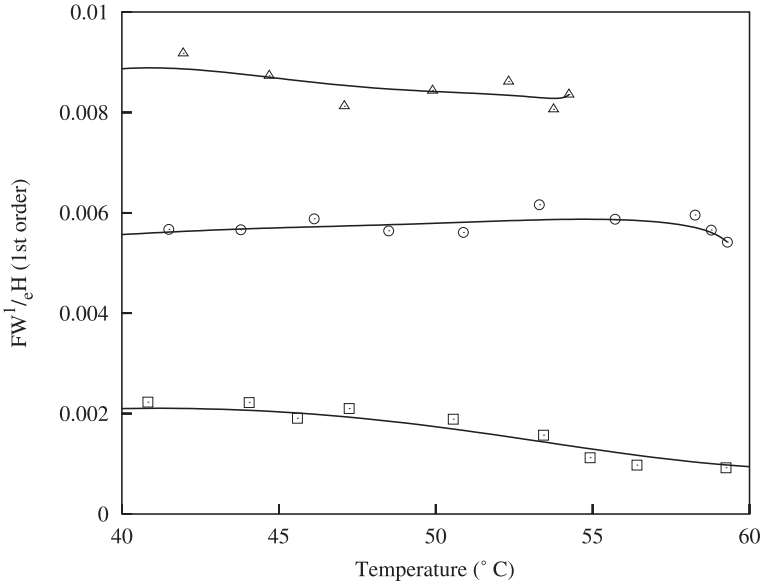


Fig. 3. Width of the first-order Bragg diffraction peak of MLVs of DOPE-Me (△) and DOPE-Me with either 2 (□) or 5 (○) mol% CBZ-D-FFG, as a function of temperature. FW1/eH is the full width of the fitted Lorentzians at 1/e (e = 2.718) height.

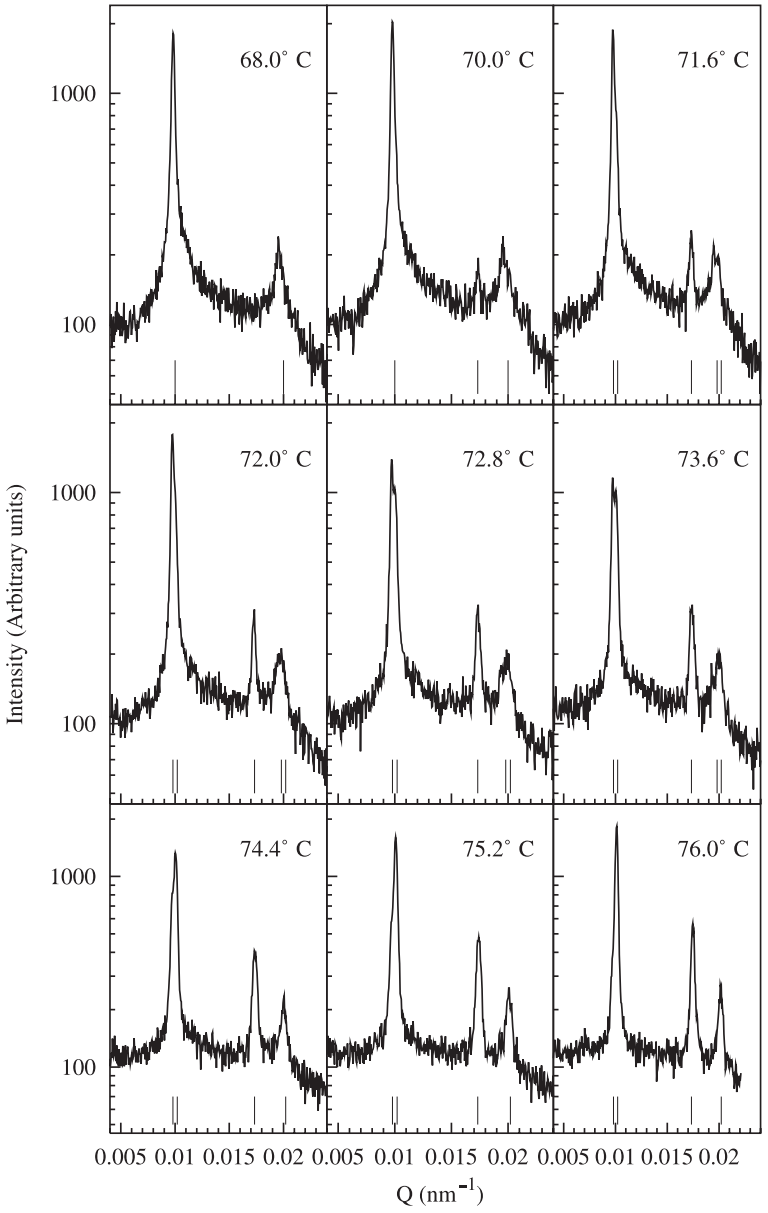


Fig. 4. X-ray diffraction profiles of multilamellar vesicles composed of DOPE-Me plus FeLV fusion peptide (1 mol%) at specific temperatures. The diagram clearly shows the emergence of the (110) peak at 70°C, which is followed by splitting of the (100) and (200) reflections as the hexagonal phase develops.

reflection, or a discontinuity in the position of the first order. Also, the first orders of lamellar and hexagonal are so much stronger than higher order cubic peaks as to be easily identifiable.

### 3.1. DOPE-Me and p15EK

The SAXS data for the pure lipid controls were in agreement with previously published results [8,18]. An 'ordered' transition [19] was observed for the pure lipid at approximately 60°C where $L_\alpha$ and $H_{II}$ phases coexist (Fig. 1A,B). The lamellar $d$-repeat ($d_L$) tended to increase with temperature due to sample disorder. The calculated hexagonal $d$-repeat ($d_H$) steadily decreased after its formation due to increased hydrocarbon chain splay at higher temperatures, which facilitates tighter headgroup packing.

Fig. 1D–F shows the typical mesomorphic behav-

iour for DOPE-Me with 1 mol% p15EK. As previously shown [2,3], p15EK is a potent inducer of inverted lipid structures, witnessed by the early onset of the hexagonal phase as well as two cubic phases.

### 3.2. CBZ-D-FFG

The structural effects of CBZ-D-FFG on DOPE-Me phase behaviour are significant, as seen in Fig. 1A–C. Firstly, adding CBZ-D-FFG increases the lamellar repeat $d_L$, to 6.3 nm in the 2 mol% and 6.7 nm in the 5 mol% samples. Secondly, the peptide causes premature $L_\alpha$ breakdown, at 58°C and 54°C in the 2 mol% and 5 mol% samples, respectively (see Fig. 2). After $L_\alpha$ decay, no coherent scattering is observed until higher temperatures. At 68°C, both strong hexagonal and weak cubic phases are observed. The unit cell size of the hexagonal phase is reduced as a function of increasing CBZ-D-FFG content. Interestingly, no diffraction is observed with the 10 mol% sample regardless of temperature.

The effect of CBZ-D-FFG on the $L_\alpha$ phase was examined further by analysing the full-width of the fitted Lorentzians at 1/e (e = 2.718) height (FW1/eH). The FW1/eH value is a useful estimate of sample disorder [20]. Values for the first-order reflections for MLVs with and without CBZ-D-FFG are shown in Fig. 3. The $L_\alpha$ reflections become progressively broader as the concentration of CBZ-D-FFG increased, indicating that CBZ-D-FFG destabilised the $L_\alpha$ phase in a concentration-dependent manner.

Fig. 1G–I shows the effect of adding 1 mol% p15eK to MLVs of DOPE-Me with CBZ-D-FFG. The fusion peptide stabilises isotropic structures at the expense of hexagonal phase. Two different cubic phases were observed for each concentration of CBZ-D-FFG, although their onset increased with temperature in a concentration-dependent manner. The two cubic phases are consistent between the three different CBZ-D-FFG concentrations, that is, the same orders appear with the same ratios. Note that, in the presence of p15EK, cubic structures were even observed with the CBZ-D-FFG 10 mol% sample. The lattice repeat distance ($d_Q$) decreases by approximately 8 nm between onset and 70°C. In addition, the fusion peptide negates the large $d_L$ increase of the 5 mol% CBZ-D-FFG.

### 3.3. LPC

LPC at 1 mol% had a similar effect on the phase behaviour of DOPE-Me to 2 mol% CBZ-D-FFG. The onset of the hexagonal phase was observed at a comparable temperature although, in the presence of LPC, the $L_\alpha$ phase persists to higher temperatures. In addition, $d_L$ and $d_Q$ are similar for both samples. Fig. 4 is an example of raw data that shows the transition sequence from lamellar to hexagonal. Note the appearance of the (110) peak at 70°C, which is followed by splitting of the (100) and (200) reflections as the hexagonal phase develops. The largest difference, however, between the two in-

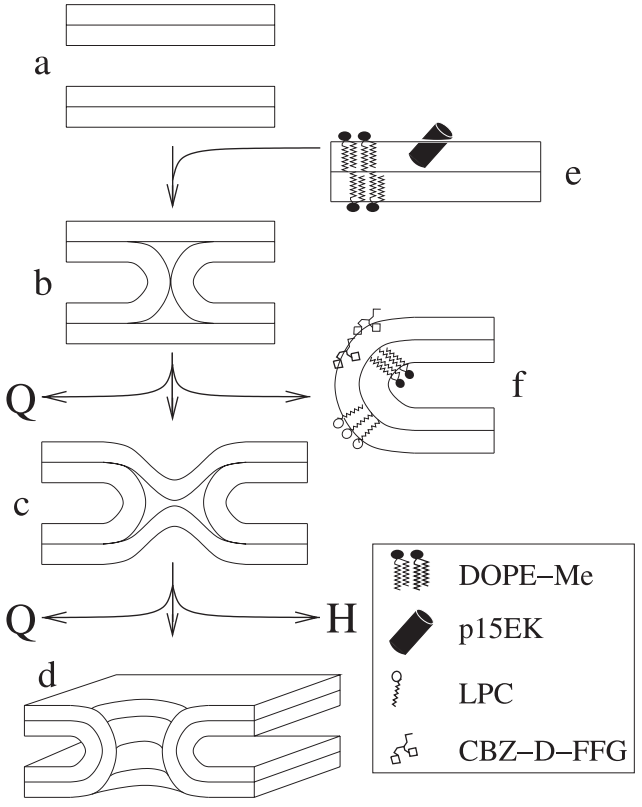


Fig. 5. An illustration of the stalk theory of membrane fusion, showing the commonly accepted intermediates: opposing bilayers (a), stalks (b), hemifusion structure (c) and fusion pore (d). The figure has been expanded to incorporate the findings of this study. The oblique insertion of fusion peptide (e) facilitates formation of stalks by lipid disruption. Fusion inhibitors interfere with an early stage of the fusion pathway (a–d), and/or the lamellar to hexagonal pathway, by reducing negative curvature (f).

hibitors is that no cubic phase was observed in the presence of LPC.

In the presence of 1 mol% p15EK the $L_\alpha$ phase persists until 69°C, somewhat less than with LPC alone. However, $d_L$ is exactly the same with or without the fusion peptide, 0.2 nm larger than pure DOPE-Me, and 0.1 nm larger than p15EK alone. Whereas p15EK lowered the onset of hexagonal phase for pure lipid, in the presence of LPC, it increases the onset, suggesting that the type of hexagonal phase is different. The most marked difference is that LPC increases $d_Q$, compared to p15EK alone, by a dramatic 10 nm. The onset is also at higher temperature.

## 4. Discussion

The results raise interesting topics for debate with regard to monolayer curvature (especially in the fusion process) and membrane stability. Fusion theory has been covered in detail by a number of authors (e.g., [3,5,21]); Fig. 5a–d illustrates the current thinking. Two opposed bilayers are first brought near to each other, either through thermal fluctuations or by the action of fusion proteins. The *cis* leaflets of the opposing bilayers merge to form a so-called stalk structure. Stalks can then grow in diameter until the *trans* leaflets touch forming a hemifusion structure, also called a transmembrane contact or TMC. These structures then can either open into fusion pores or aggregate to form precursors for the $H_{II}$ phase. Fusion pores can further aggregate to form a cubic phase or expand until fusion is complete.

However, the exact location and role of fusion peptides have yet to be determined in the theoretical considerations of these idealised lipidic structures. The data above suggest that p15EK promotes negative curvature, but how exactly does it do this? Furthermore, even in the absence of an intact hinge mechanism, such as found in haemagglutinin of influenza or gp41 of HIV, how do fusion peptides such as p15EK catalyse the first step of the whole process, in which two bilayers are brought together? This is evidenced by the lowering of the $L_\alpha$–$H_{II}$ transition, which requires overcoming the repulsive interbilayer van der Waals forces at a lower thermal energy.

We recently reported unique direct evidence for the insertion of another fusion peptide into membranes at an oblique angle [22]. This mode of insertion leads naturally to the proposal that a likely consequence is the destabilisation of membrane bilayers and direct promotion of monolayer mixing [23]. This is shown diagrammatically in Fig. 5e.

In order to bridge the conceptual gap between observations of obliquely-inserting peptides and the membrane fusion, it may help to concentrate less on the bulk properties of membranes and more on the molecular events taking place in the phospholipids surrounding individual fusion peptide molecules. The smooth curves seen in diagrams (e.g., Fig. 5) are unlikely to be a true representation of monolayers actually undergoing fusion. Although the overall effect of fusion peptide insertion may be described as a net increase in negative curvature (hence the appearance of cubic phases), a closer look is likely to reveal numerous discontinuities in molecular packing. This, in part, avoids the problem of the high energy of stalk formation predicted by current theory [3,21]. In short, there may not be a simple, closed form of geometry for the fusion intermediates, from which the free energy can be calculated by the Helfrich equation [24].

Despite all this, the total phase diagram for our lipid/fusion peptide/inhibitor system, shown in Fig. 2, can be related to a mechanism of fusion. The first task is to properly identify the types of the non-lamellar phases. Due to Babinet's principle, it is impossible for diffraction techniques to distinguish type I (oil-in-water) and type II (water-in-oil, or inverted) structures, making phase identification difficult. However, from previous knowledge of lipid polymorphism and the effects of LPC and CBZ-D-FFG on bilayers, we can reason what phases are being induced and their importance in the fusion process.

A well-known characteristic of PE lipids is their propensity to form inverted $H_{II}$ phases [3,8,25,26]. DOPE-Me is characterised by the methyl group on the ethanolamine headgroup and the low melting temperature, highly fluid, oleoyl chains. These molecular attributes contribute to the relatively stable lamellar phase of this lipid at biological temperatures, in comparison to most other PE lipids. However, this should not affect the nature of the lamellar to hexagonal transition, so we expect this to also be of type $L_\alpha$–$H_{II}$.

The effect of p15EK on MLVs of DOPE-Me is to lower the lamellar to hexagonal transition and induce new cubic phases. At this reduced $T_H$ there is less thermal energy available for making stalks than in the pure lipid. The extra work must therefore come from disruption of the lipid packing by the peptide (Fig. 5e). It is reasonable to assume that the hexagonal phase is $H_{II}$, since there is no significant change in $d_H$ or $T_H$ from the pure lipid.

The hexagonal and cubic phases coexist over a broad temperature range and it is quite possible that the p15EK does not partition equally between them. Since the fusion peptide promotes the formation of cubic phases [8], it is possible that it partitions preferentially there. It seems to be characteristic of p15EK to induce two separate cubic phases (see Fig. 1F,I). There is inherent difficulty in trying to identify the specific space group of a cubic phase [27], but this may not be a major concern. Interestingly, each of the two phases never varies significantly in $d_Q$ or $T_Q$. We tentatively assign both phases as being inverted, or type $Q_{II}$. p15EK belongs to the class of amphipathic peptides that insert obliquely into lamellar bilayers. In the highly curved monolayers of the cubic phase the nature of the peptide–lipid interaction is an open question. Could a cubic phase maintain its symmetry if the peptide were still obliquely inserted? Has it dissociated from the membrane completely? Until more is known about specific molecular interactions in the different lipid phases, all that can be said is that the importance of p15EK in the fusion process is the promotion of inverted structures.

The characteristic molecular shape of the surfactant LPC causes it to form type I micelles, a property that has been proposed as the basis of its anti-viral activity [28]. LPC is miscible with DOPE-Me, and no phase separation was observed in these SAXS measurements. Conceptually, this system is easier to visualise with the curvature strain model of membrane fusion. We might expect the addition of LPC to counterbalance the curvature energy of pure DOPE-Me bilayers and form a more stable lamellar phase at higher temperatures. As expected, LPC retards the $L_\alpha$–$H_{II}$ transition by 4°C and stabilises the lamellar for another 15°C.

Fourier transform infrared studies have shown that LPC can alter the angle of peptide insertion into the bilayer, such that an otherwise obliquely-inserting peptide inserts at an angle perpendicular to the bilayer surface [29]. If LPC is altering the orientation of p15EK, then the late, post-cubic, appearance of a hexagonal phase indicates it might be of type I. In the presence of LPC, the large radius ($d_Q$ = 20–30 nm) of the cubic indicates that this was type II. Although LPC prefers type I structures, it requires them to be much smaller. As we have mentioned, molecular interactions such as the insertion of a large peptide may account for the difficulties of a continuum model of fusion. So, although we can calculate the induced decrease in curvature strain from the measured repeat spacings, molecular interactions must play a more significant role in the entire process.

The sequence for CBZ-D-FFG is taken from the conserved N-terminal region of F1 protein of the paramyxovirus family. It has been shown that CBZ-D-FFG inhibits fusion of DOPE-Me vesicles [10] and inhibits the infectivity of several viruses, including Sendai, SV5 and measles [30]. As shown in Fig. 2, increasing the concentration of CBZ-D-FFG causes the breakdown of the lamellar phase well before the formation of a non-lamellar phase. For each sample, there was a temperature range where no diffraction was observed before the onset of the hexagonal phase and cubic phase. Fig. 3 shows the increased sample disorder expressed as the width of the first order diffraction peak. No diffraction at all was observed with 10 mol% CBZ-D-FFG, indicating complete micellisation of the lipid.

The observed increase in $d_L$ may be a factor involved in membrane destabilisation by CBZ-D-FFG. The unit cell size is dependent on two tail-to-tail lipid molecules and the associated interfacial water molecules. Phenylalanine in membrane proteins is often associated with the hydrophobic–hydrophilic interface, which would place CBZ-D-FFG at the membrane surface. However, we would then expect to see a decrease in $d_L$ from membrane thinning instead of the observed increase. Furthermore, CBZ-D-FFG is not charged so it would not be expected to draw extra water between the bilayers. Previous studies have argued that the binding affinity of CBZ-D-FFG to lipid molecules is enhanced with large positive curvature [11,13,31]. Therefore, we believe that CBZ-D-FFG breaks down the MLVs into oil-in-

water (type I) micelles before transforming into an $H_I$ phase. This argument is supported by the observation that increasing CBZ-D-FFG content reduces the unit cell size of both the hexagonal and cubic phases. Increasing the concentration of CBZ-D-FFG causes the breakdown of $L_\alpha$ into micelles at progressively lower temperatures until the 10 mol% sample forms micellar dispersions at room temperature.

The mechanism of bilayer breakdown by CBZ-D-FFG may be related to its ability to inhibit membrane fusion. The $H_{II}$ phase, favoured by p15EK is eliminated at all concentrations of CBZ-D-FFG. However, the cubic phases are similar in $d_Q$ and $T_Q$ to that found with just the peptide present, indicating that they might be $Q_{II}$. The SAXS data reveal that, at a concentration of 5 mol%, CBZ-D-FFG causes the coexistence of two lamellar phases. One of these phases has an increased $d_L$, somewhat similar to the single lamellar phase seen at the same level of CBZ-D-FFG, in the absence of peptide. At 10 mol% no lamellar scattering was again observed, although the peptide caused the formation of cubic phases of a similar $d_Q$, but higher $T_Q$. This leads to the suggestion that the inhibitor partitions preferentially into the larger and/or flatter structures and the peptide into smaller/negatively curved structures. CBZ-D-FFG and p15EK appear to compete for lipid binding. However, the modes with which they interact with lipid molecules are incompatible with each other.

A pattern is emerging from the above discussion. Both fusion inhibitors presented here inhibit inverted phases in general and the $H_{II}$ phase in particular, however in contrasting ways. Although we have presented this analysis in terms of monolayer curvature, this approach is more useful in the case of LPC. The addition of LPC to DOPE-Me alters the structural characteristics of the bilayer to reduce the efficiency of the fusion peptide. In contrast, the mechanism of inhibition by CBZ-D-FFG primarily involves protein–lipid interaction.

Regardless of mechanism, inhibition of fusion seems to benefit from the prevention of $H_{II}$ precursors. One of the earliest precursors is the hemifusion structure (Fig. 5c), which is the most logical structure before a fusion pore and ultimately, complete fusion. If the fusion process were to be arrested at this point or before (Fig. 5f), neither fusion nor $H_{II}$ phases could occur. However, cubic phases could still occur because of the numerous spacegroups available that do not rely upon these intermediates [32]. This agrees with the data presented here and opens new avenues of investigation. We believe that further progress would be made by determining the location and orientation of the fusion promoters and inhibitors within non-lamellar structures.

## Acknowledgements

Grateful thanks are extended to Dr Heinz Amenitsch at Sincrotrone Trieste Elettra and Dr Gunter Grossman at Daresbury SRS for their expert technical assistance, and Ms S. Darkes for commenting on the manuscript. This work was supported by grants from the Wellcome Trust, the Central Laboratories of the Research Councils (CLRC) and the European Community HPP-TAMRI Program.

## References

[1] J.M. White, Annu. Rev. Physiol. 52 (1990) 675–697.
[2] S.M.A. Davies, R.F. Epand, J.P. Bradshaw, R.M. Epand, Biochemistry 37 (1998) 5720–5729.
[3] M.J.M. Darkes, S.M.A. Davies, J.P. Bradshaw, FEBS Lett. 461 (1999) 178–182.
[4] L.V. Chernomordik, J. Zimmerberg, Curr. Opin. Struct. Biol. 5 (1995) 541–547.
[5] D.P. Siegel, Biophys. J. 76 (1999) 291–313.
[6] V.S. Markin, M.M. Kozlov, V.L. Borovjagin, Gen. Physiol. Biophys. 5 (1984) 361–377.
[7] R. Jahn, T.C. Südhof, Annu. Rev. Biochem. 68 (1999) 863–911.
[8] T.J. McIntosh, K.G. Kulkarni, S.A. Simon, Biophys. J. 76 (1999) 2090–2098.
[9] D.R. Kelsey, T.D. Flanagan, J.E. Young, P.L. Yeagle, Virology 182 (1991) 690–702.
[10] D.R. Kelsey, T.D. Flanagan, J.E. Young, P.L. Yeagle, J. Biol. Chem. 265 (1990) 12178–12183.
[11] P.L. Yeagle, J. Young, S.W. Hui, R.M. Epand, Biochemistry 31 (1992) 3177–3183.
[12] A.R. Dentino, B. Westermann, P.L. Yeagle, Biochim. Biophys. Acta 1235 (1995) 213–220.
[13] R.M. Epand, Biosci. Rep. 6 (1986) 647–653.
[14] R.M. Epand, Biochemistry 24 (1985) 7092–7095.
[15] L.V. Chernomordik, M.M. Kozlov, G.B. Melikyan, I.G. Abidor, V.S. Markin, Yu.A. Chizmadzhev, Biochim. Biophys. Acta 812 (1985) 643–655.

[16] L.V. Chernomordik, Chem. Phys. Lipids 81 (1996) 203–213.
[17] R.D.B. Fraser, T.P. MacRae, Int. J. Biol. Macromol. 3 (1981) 193–200.
[18] S.M. Gruner, M.W. Tate, G.L. Kirk, P.T. So, D.C. Turner, D.T. Keane, Biochemistry 27 (1988) 2853–2866.
[19] A. Colotto, I. Martin, J. Ruysschaert, A. Sen, S.W. Hui, R.M. Epand, Biochemistry 35 (1996) 980–989.
[20] A.E. Blaurock, J.C. Nelander, J. Mol. Biol. 103 (1976) 421–431.
[21] P.I. Kuzmin, J. Zimmerberg, Y.A. Chizmadzhev, F.S. Cohen, Proc. Natl. Acad. Sci. USA 98 (2001) 7235–7240.
[22] J.P. Bradshaw, M.J.M. Darkes, T.A. Harroun, J. Katsaras, R.M. Epand, Biochemistry 39 (2000) 6581–6585.
[23] R. Brasseur, M. Vandenbranden, M. Cornet, A. Burny, J. Ruysschaert, Biochim. Biophys. Acta 1029 (1990) 267–273.
[24] W. Helfrich, Z. Naturforsch. Sect. C Biosci. 28C (1973) 693–703.
[25] J. Gagné, L. Stamatatos, T. Diacovo, S.W. Hui, P. Yeagle, J. Silvius, Biochemistry 24 (1985) 4400–4408.
[26] H. Ellens, D.P. Siegel, D. Alford, P.L. Yeagle, L. Boni, L.J. Lis, P.J. Quinn, J. Bentz, Biochemistry 28 (1989) 3692–3703.
[27] J.M. Seddon, R.H. Templer, in: R. Lipowsky, E. Sackmann (Eds.), Handbook of Biological Physics, Vol. 1, Elsevier Science, Amsterdam, 1995, pp. 97–160.
[28] N. Fuller, R.P. Rand, Biophys. J. 81 (2001) 243–254.
[29] I. Martin, M.C. Dubois, T. Saermark, R.M. Epand, J. Ruysschaert, FEBS Lett. 333 (1993) 325–330.
[30] C.D. Richardson, A. Scheid, P.W. Choppin, Virology 105 (1980) 205–222.
[31] D.C. Turner, M. Straume, M.R. Kasimova, B.P. Gaber, Biochemistry 34 (1995) 9517–9525.
[32] J.M. Seddon, Biochim. Biophys. Acta 1031 (1990) 1–69.